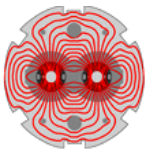

LHC Project Note 407

2007-07-09

Igor.Baichev@cern.ch

Proton Losses in the LHC due to Momentum Cleaning at Top Energy

I. Bayshev / TS-LEA and IHEP-Protvino

Keywords: proton, collimator, cleaning, momentum, scattering, losses

Summary

A set of the simulations of the momentum cleaning during collisions at top energy is done. The results for the proton losses at the collimators and at the other limiting apertures are presented and discussed.

1. Introduction

The collimation system of LHC is to intercept both the transverse halo of the beams and the off-momentum protons outside the RF bucket. To reach these goals it consists of the two parts. The betatron cleaning insertion IR7 houses the betatron collimators and the momentum cleaning insertion IR3 houses the momentum collimators. The tertiary collimators protecting the inner triplets in the experimental insertions IR1, IR2, IR5 and IR8 are also in the baseline. Thus proton losses are concentrated at the collimators to prevent radiation induced quenches of the superconducting magnets both in the arcs and insertions.

The collimation system is described in the LHC Design Report [1]. The basics of the two-stage collimation are given in [2, 3] and the features of the momentum cleaning are explained in [4, 5]. Numerical simulations are necessary to estimate the loss distribution between the collimators and the losses at the other elements for the given machine layout, optics and mechanical apertures. Losses in the experimental insertions are the most interesting as the source term for the background estimations like those reported in [6].

Scattering in the collimators as the main mechanism of losses in the machine is discussed in this paper from the optical point of view. Detailed simulations of the momentum cleaning are described and the resulting losses due to momentum cleaning are presented.

2. Momentum cleaning optics

The optical betatron functions $\beta(s)$ and $\alpha(s)=-\beta'(s)/2$, betatron phase advance $\mu(s)=\int ds/\beta(s)$, the dispersion function $D(s)$ and its derivative $D'(s)$ describe the single particle transverse motion in the frame (x,y,s), where s is the longitudinal coordinate, x and y are the horizontal and vertical transverse coordinates. The horizontal betatronic *rms* size of the beam with the emittance ε is expressed through the β-function as $\sigma_x = (\varepsilon\cdot\beta_x)^{1/2}$. The normalized coordinates are defined as $X = x/\sigma_x$ and $X' = (\alpha_x x + \beta_x x')/\sigma_x$ so that the horizontal betatron motion is reduced to the motion in the phase plane (X, X') along the circular trajectory with the radius $A_x = (X^2 + X'^2)^{1/2}$. For example, the transfer of a particle from s_1 to s_2 is a simple rotation

$$X_2 = X_1\cdot\cos\mu + X_1'\cdot\sin\mu, \quad X_2' = X_1'\cdot\cos\mu - X_1\cdot\sin\mu\,,$$

where $\mu = \mu_x(s_2) - \mu_x(s_1)$. The amplitude A_x is an invariant i.e. it does not depend on s. The complete trajectory of the proton with the nonzero relative momentum offset $\delta = 1 - p/p_0$ consists of both the betatronic and chromatic parts as follows

$$x(s) = x_\beta(s) - D_x(s)\cdot\delta \ , \ x'(s) = x'_\beta(s) - D_x'(s)\cdot\delta \, .$$

The vertical motion is described in the same way though the vertical dispersion is normally much smaller than the horizontal one.

The energy spread of the beam protons is limited by the size of the RF bucket (the half height δ_B is equal to $3.6\cdot10^{-4}$ at top energy). The off-momentum protons with $\delta>\delta_B$ lose their energy due to synchrotron radiation at a rate 6.71 keV ($9.6\cdot10^{-10}$ units of δ) per turn until δ gets close to the momentum aperture $\delta_{cut} = -x_{col}/D_x$ of the primary momentum collimator with the jaw at $x=x_{col}$. These protons keep the betatronic amplitude which they had being inside the beam. The proton touches the collimator when $X_\beta\cdot\sigma_x - D_x\cdot\delta = x_{col}$, $X_\beta = -A_x$, $X'_\beta = 0$. Thus $\delta = \delta_{cut} - A_x\cdot\sigma_x/D_x$ and the spectrum of protons touching the primary jaw can be obtained from the amplitude distribution of the beam protons

$$dn/dA_x = A_x\cdot exp(-A_x^2/2) \,/\, [1 - exp(-A^2_{max}/2)]$$

with the amplitude cut A_{max} equal to 3 or even to 2.5. The most probable value of A_x is close to 1 and therefore the most probable $\delta = \delta_{cut} - \sigma_x/D_x$.

The primary impact parameter $b = |x - x_{col}|$ is small compared to σ_x = 257 μm at the primary momentum collimator. The distributions of b were studied in [7] for the beginning of the acceleration ramp. The results of the SIXTRACK simulations were approximated there by an exponential function $dn/db = exp(-b/b_0)/b_0$ with the slope b_0 in the range 4 μm – 10 μm. In the case of collisions at top energy the values of b_0 must be a factor of ~4 smaller due to the smaller beam size.

Scattering in the collimator jaw increases the parameter of the subsequent impacts. Energy loss simply moves the centre point of the betatronic oscillations towards the jaw. The change of the angle from x_0' to x' increases the amplitude from A_0 to $A_0 + a$ with the amplitude increment $a = (A_0^2+\Delta^2)^{1/2} - A_0$, where $\Delta = (x - x_0')\cdot\beta_x/\sigma_x$ is the normalized angle of scattering. Scattering shifts also the betatronic phase from $-\pi$ to $-\pi + \varphi_s$, where $\sin(\varphi_s) = \Delta/(A_0+a)$. If a is large enough then the proton can enter one of the other collimators and be absorbed or scattered there. If $a<1$ then it will certainly come back to the primary jaw after a number of full turns in the machine. This number of turns will be the larger the smaller is a/A_0.

Scattering in the vertical plane increases the vertical betatronic amplitude when the normalized scattering angle $\Delta_Y = (y' - y_0')\cdot\beta_y/\sigma_y$ satisfies the condition $\Delta_Y^2 + 2\cdot\Delta_Y\cdot Y_0' > 0$. Thus scattering in the essentially horizontal primary momentum collimator can lead to the losses at the vertical betatron collimators or at the vertical tertiary collimators in the experimental insertions.

The collimator surface can be presented as a line tangent to the circle of a radius n in the frame (X, Y) with the centre at the beam orbit. For example n=1 means that the half-gap of a purely horizontal collimator is equal to $1\sigma_x$ or it is equal to $1\sigma_y$ in the case of a purely vertical collimator. Historically, the notation n_1 was assigned to the primary collimators TCP and n_2 to the secondary ones TCSG. Later n_3 was added for the tertiary collimators TCT and here we add the notation n_A for the active absorbers TCLA in the cleaning insertions. In the momentum collimation system at top energy n_1=15, n_2=18, n_A=20 for the horizontal absorbers and n_A=10 for the vertical one. For the betatron collimators n_1=6, n_2=7 and n_A=10 for all the absorbers. The tertiary collimators are set to n_3=8.3 at the nominal collision optics and we will use the

same n_3 for the early collision optics. There is also the single horizontal jaw TCDQ in IR6 at n=10.

3. Simulations

The STRUCT code [8] is used in this work for the simulation of the momentum cleaning to calculate the losses in the machine. It consists of the scattering and tracking routines. The relevant scattering routines simulate the proton transport in the collimator jaw. Multiple Coulomb scattering is simulated as a continuous process with the account of the proton position and direction with respect to the collimator jaw surface. Ionisation energy loss is also a continuous process. The point-like events are absorption and scattering. Absorption is meant to be the inelastic nuclear interaction without production of protons with δ<0.3. Diffractive and non-diffractive production of protons with δ<0.3 is the inelastic scattering. The nuclear elastic scattering is coherent (on the entire nucleus) and incoherent (on the nucleons).

The tracking routines realize the "thick lens" δ-dependent transport maps of the accelerator elements which are dipole, quadrupole, sextupole and drift space. The elements sequence, lengths and magnetic field parameters ("k-values") defining the machine layout and optics are taken as the input from the MAD output. The optics version 6.5 is used in this work. The lattice functions calculated by STRUCT are in a good agreement with those calculated by MAD. The other example of a good agreement is shown in Figure 1.

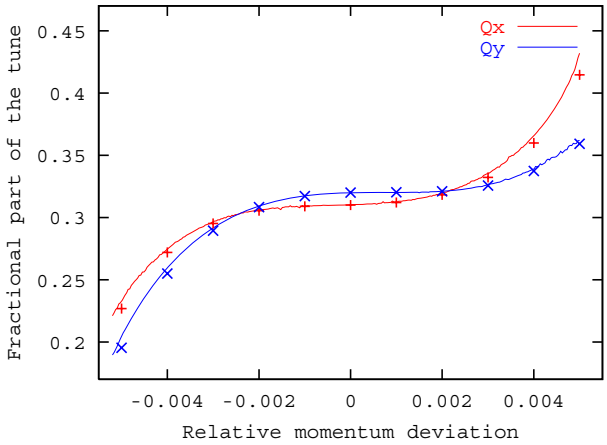

Figure 1 The momentum dependence of the LHC tune for the nominal collision optics. The relative momentum deviation is equal here to $-\delta$. Lines in the plot present the results of the current version of STRUCT, symbols are the results of MADX - courtesy of Thys Risselada.

The on-momentum orbit and β-functions are calculated first for the proper positioning of the collimators. The example of the on-momentum and off-momentum horizontal trajectories of the protons with zero betatronic amplitude is given in Figure 2. Obviously for the on-momentum proton x=0 everywhere except for IR5 and IR8 where the orbit bump produces the horizontal crossing of the beams. The off-momentum trajectory follows the horizontal dispersion function $D_x(s)$ everywhere except for the orbit bumps in IR5 and IR8. The nonzero dispersion at the betatron collimators must be noted separately. The half-gap of the horizontal primary collimator TCP.C6L7 is $6\sigma_x$ = 1.65 mm and the dispersion there is D_x = 0.59 m. Therefore the primary momentum halo can be cut by this betatron collimator at $\delta = 2.8 \cdot 10^{-3}$ in the hypothetic case of fully open momentum collimators.

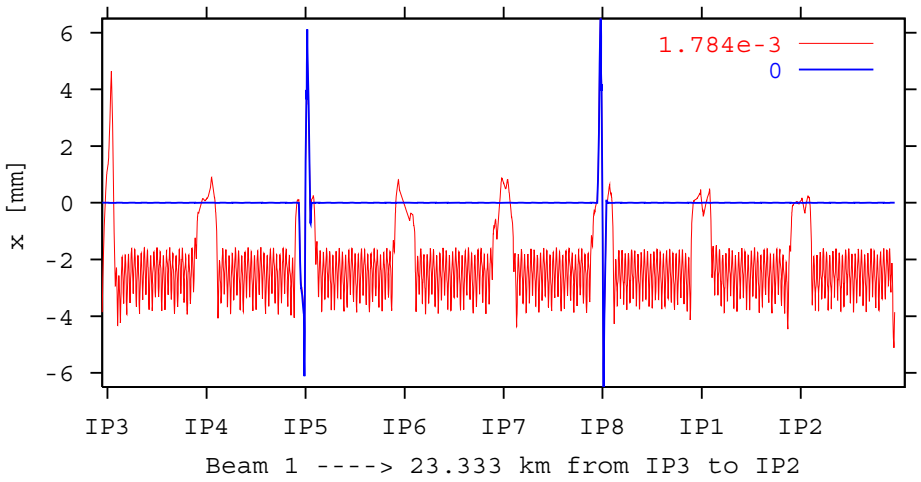

Figure 2 The on-momentum ($\delta = 0$) and the off-momentum ($\delta=\delta_{cut} = 1.784\cdot10^{-3}$) proton trajectories for the nominal collision optics Beam1.

The simulation of a single event of momentum cleaning starts from the proton impact at the jaw of the primary momentum collimator TCP and its transport in the jaw material. If proton is not absorbed in the jaw then the element by element and turn by turn tracking is being done. During tracking the proton can enter the jaw of another collimator or get back to the primary jaw. In this case the transport in the material is simulated again. The cleaning event is accomplished when the proton is absorbed in one of the jaws or reaches the limiting aperture of one of the other elements.

3.1 Preliminary studies

As it is shown above the exponential function with the slope b_0~1μm can be reasonably used as the distribution of the primary impact parameter. At the same time it is important to understand how sensitive the simulation results can be to the primary impacts. Three low statistics runs were done for the nominal collision optics of Ring 1 varying the slope b_0. In addition to the loss registration the angles of scattering in the primary jaw were recorded to calculate the horizontal amplitude increment of every scattering. As it is seen from the Table 1

Table 1: Loss distribution from the "low statistic" runs of 100000 cleaning events each.

b_0 [μm]	entire IR3	TCP in IR3	IR7	IR5	IR1+IR2+IR8
0.1	92347	77906	7382	219	52
1.0	92190	77862	7525	243	42
10	92284	78103	7445	224	47

less than 8% of protons are lost outside the momentum cleaning insertion mostly at the betatron collimators in IR7. The most important result is that the loss distribution does not depend significantly on the primary impact parameters. This does not mean that the cleaning process is not sensitive to the primary impact at all. The smaller the impact parameter is the smaller is the proton path inside the material of the primary jaw and therefore the smaller is a single pass probability of nuclear interaction. This probability is accumulated impact by impact. When the interaction occurs the proton is either absorbed or scattered at an angle which does not depend on the path length. Therefore the large increments of the betatronic amplitude do not depend on

the impact parameters. This fact is illustrated in Figure 3 where the calculated distributions of the amplitude increment are shown.

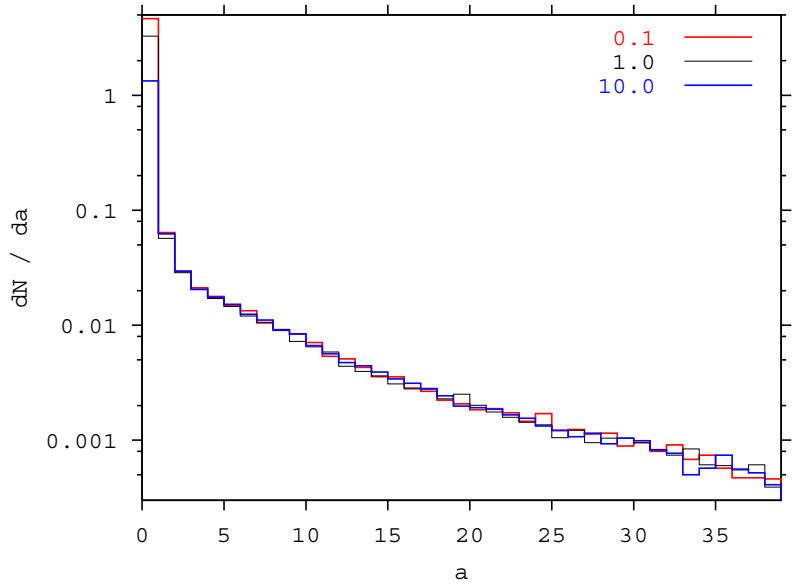

Figure 3 The distributions of the amplitude increment a due to the scatterings in the primary momentum collimator for the different slopes b_0 of the exponential distribution of the primary impacts. The values of b_0 [μm] are given in the plot.

Note that these are not single pass distributions. Their integral over the range $(0, \infty)$ of a is the average number N_s of scatterings in the primary collimator per cleaning event. N_s is equal to 4.90, 3.51 and 1.58 for $b_0 = 0.1$ μm, $b_0 = 1$ μm and $b_0 = 10$ μm respectively. This dependence of N_s on b_0 results from the small a part of the histograms and the integral over the range $(1, \infty)$ is equal to approximately 0.25 for any of the three values of b_0.

3.2 Momentum cleaning rates

The special study to predict the annual losses in the LHC is described in [9]. All the necessary beam parameters and operational scenarios are given there so that the annual losses assigned to the momentum collimation system can be converted to the momentum cleaning rates during both the nominal physics and the early physics. Our conversion results in the following rates: $\mathbf{4.3 \cdot 10^8}$ p/s for the nominal physics and $\mathbf{1.2 \cdot 10^8}$ p/s for the early physics.

4. Loss distributions

The main set of simulations is done with the statistics of 10^7 cleaning events per run and b_0=1μm. Four runs correspond to the two optics (nominal collision and early collision) and two beams. The complementary set of four runs is similar to the main one except for the fully open tertiary collimators in the experimental insertions. The losses at the collimators and at the other elements are given below per 1 cleaning event except for Figure 7 where the absolute loss rates at the tertiary collimators are shown. The loss densities below are the losses per unit of the element length per one cleaning event. Any of the numbers given per one cleaning event can be easily converted to the loss rates being multiplied by the cleaning rates.

The loss distributions along the LHC are shown in Figures A1 – A4 of the Appendix, Figures A3 and A4 being the same as Figures A1 and A2 but for the case with the fully open

tertiary collimators. The losses at all the collimators are listed in the Table A1 of the same Appendix. Table 2 below complements Figures A1 and A2 with the integrated numerical data.

Table 2: Losses in the Insertions. The additional line for the primary momentum collimators TCP.3 is given also in the row for IR3.

	Nominal collisions		Early collisions	
	Beam 1	Beam 2	Beam 1	Beam 2
IR3	0.92254	0.95187	0.93579	0.96881
TCP.3	*0.77997*	*0.78532*	*0.80028*	*0.79586*
IR7	0.07462	0.03786	0.04933	0.02663
IR6	-	$3.6\cdot10^{-6}$	$4.02\cdot10^{-4}$	$4.7\cdot10^{-6}$
IR1	$3.67\cdot10^{-5}$	$2.49\cdot10^{-3}$	$3.86\cdot10^{-5}$	$6.80\cdot10^{-4}$
IR2	$1.18\cdot10^{-4}$	$2.67\cdot10^{-3}$	$3.97\cdot10^{-4}$	$2.86\cdot10^{-3}$
IR5	$2.49\cdot10^{-3}$	$3.99\cdot10^{-5}$	$1.378\cdot10^{-2}$	$7.5\cdot10^{-6}$
IR8	$1.91\cdot10^{-4}$	$5.06\cdot10^{-3}$	$2.57\cdot10^{-4}$	$9.98\cdot10^{-4}$

Obviously, the losses are concentrated at the collimators but not entirely.

4.1 Losses in the momentum cleaning insertion IR3

The off-momentum protons with relatively large δ are produced in the jaws of the momentum collimators. Many of them are intercepted by the active absorbers TCLA as it is seen in Figure 4, but some of them reach the aperture of the beam screen in the cold magnets of the dispersion suppressor. The peak loss density of $\approx 2\cdot10^{-4}$ m^{-1} occurs at Q8. With the quench limit of $8\cdot10^{6}$ p·m^{-1}·s^{-1} [2] we obtain the limiting cleaning rate of $4\cdot10^{10}$ p/s which is much higher than the expected operational cleaning rate of $4.3\cdot10^{8}$ p/s.

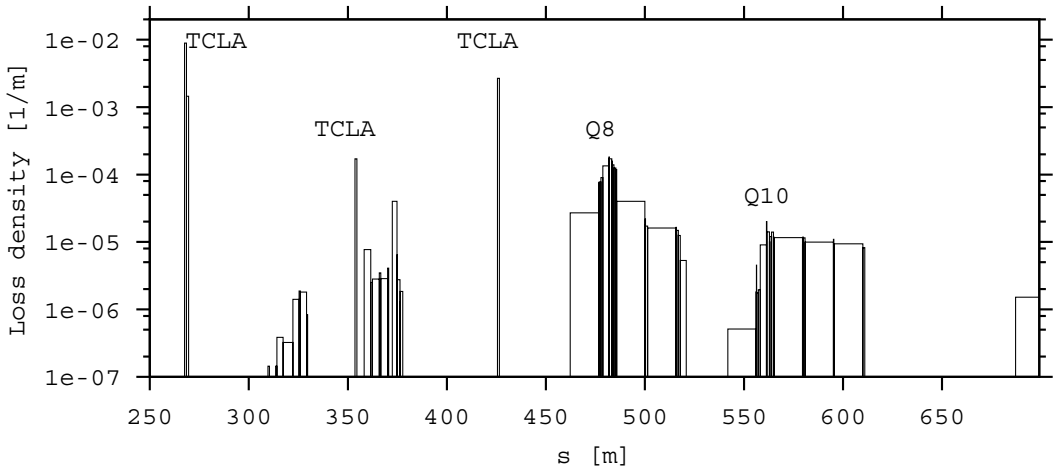

Figure 4 Loss densities in the IR3 downstream of the primary and secondary momentum collimators for the nominal collision optics Beam 1. The *s*-axis starts at the entrance of the primary collimator TCP.6L3.

For the Beam 2 (see Figure 5) the loss densities downstream of the TCLA absorbers are much lower and the peak of ~$2 \cdot 10^{-5}$ m^{-1} occurs at Q9 and Q10.

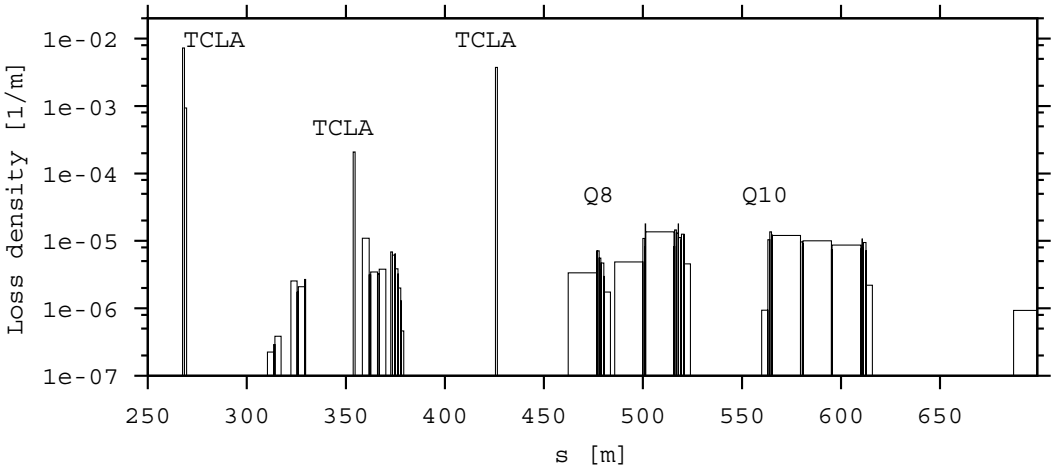

Figure 5 Loss densities in the IR3 downstream of the primary and secondary momentum collimators for the nominal collision optics Beam 2. The *s*-axis starts at the entrance of the primary collimator TCP.6R3.

The optics of IR3 in the case of the early collisions is practically the same as for the nominal collisions and the loss distributions repeat those shown above.

4.2 Losses at the betatron collimators in IR7

Losses at the betatron collimators are lower than the losses at the secondary momentum collimators but much higher than at the tertiary collimators. This means that they intercept a noticeable part of the secondary halo produced by the primary momentum collimator. An example of the impact at the betatron collimators is given in Figure 6. The relatively large

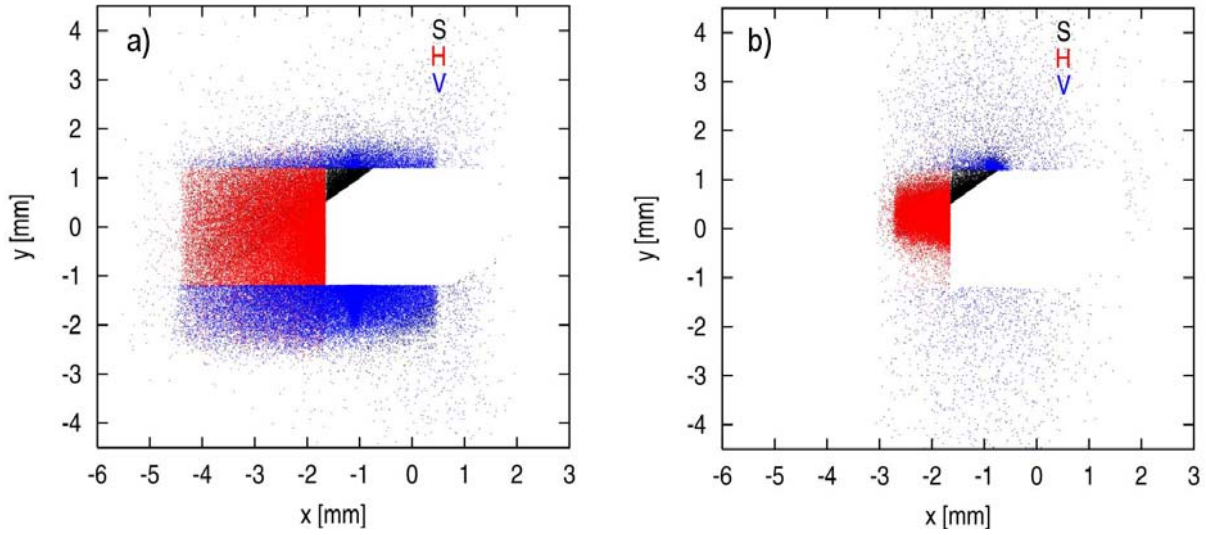

Figure 6 Impact maps of the secondary momentum halo at the primary betatron collimators – horizontal (H), vertical (V) and skewed (S) - for the nominal collision optics: a) Beam 1, b) Beam 2.

horizontal dispersion (D_x = 0.59 m for Beam 1 and D_x = 0.65 m for Beam 2) at the location of the primary betatron collimators exhibits itself in the extreme asymmetry of the impacts at the horizontal and skewed jaws. There is practically no impact at one of the two jaws of both H and S collimators. Even the impact at the vertical collimator is asymmetric due to the nonzero vertical dispersion (D_y = +0.045 m for Beam 1 and D_y = -0.186 m for Beam 2).

Dispersion is not a single reason for the asymmetries of the impact at any betatron or tertiary collimator. Screening of a collimator by the other ones is a complicated function of the betatronic phases. The momentum collimators are mostly horizontal and the asymmetry will be seen rather in the horizontal plane.

4.3 Losses in the experimental insertions

There are no other losses upstream of the experiments except the losses at the tertiary collimators. The individual numbers for each collimator can be found in the Table A1. The charts in Figure 7 show the absolute rates of losses at the pairs (horizontal + vertical) of the tertiary collimators. These rates define the source intensities for the background studies. Such a study for the betatron cleaning was done in [6] to estimate the background fluxes at IP8. The rates of $2.35 \cdot 10^6$ p/s at TCTV and $0.61 \cdot 10^6$ p/s at TCTH corresponding are reported there for

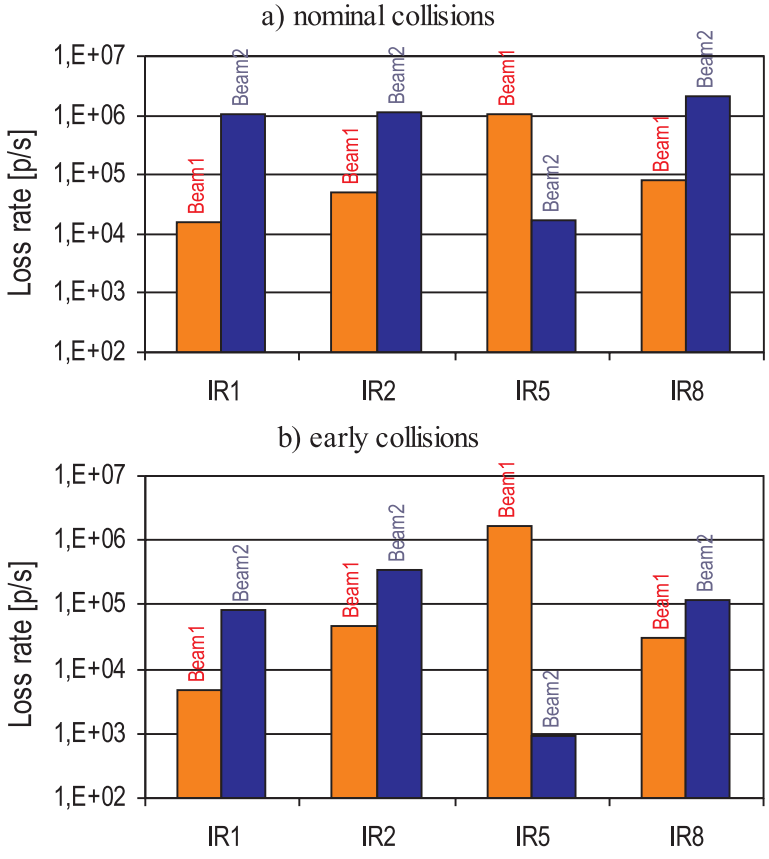

Figure 7 Loss rates at the tertiary collimators (horizontal + vertical):
a) nominal collision optics, cleaning rate of $4.3 \cdot 10^8$ p/s, b) early collision optics, cleaning rate of $1.2 \cdot 10^8$ p/s.

the betatron cleaning rate of $2.8 \cdot 10^9$ p/s. Cleaning rates in our case are lower and the rates at the same TCTH/V (IR8, Beam 1) are $\leq 10^5$ p/s though the rates of $\sim 10^6$ p/s are reached in some other IRs and in the same IR8 at the tertiary collimators of the Beam 2.

It is interesting to know the loss distribution upstream of the experiments when the tertiary collimators are fully open. Figures A3, A4 show that the highest losses in that case occur in IR5 for Beam 1 and in IR1 for Beam 2. The detailed distributions of the loss density upstream of IP5 and IP1 are shown in the Figures 8 and 9 respectively. The loss densities at the superconducting quadrupoles Q3 and Q2B are an order of magnitude lower than those at Q8 in IR3 for the case of Beam 1. In the case of Beam 2 the peak loss densities at the triplet quadrupoles of IR1 are at least twice lower than in IR3. Thus losses in the triplets do not impose any additional limitations on the momentum cleaning rate.

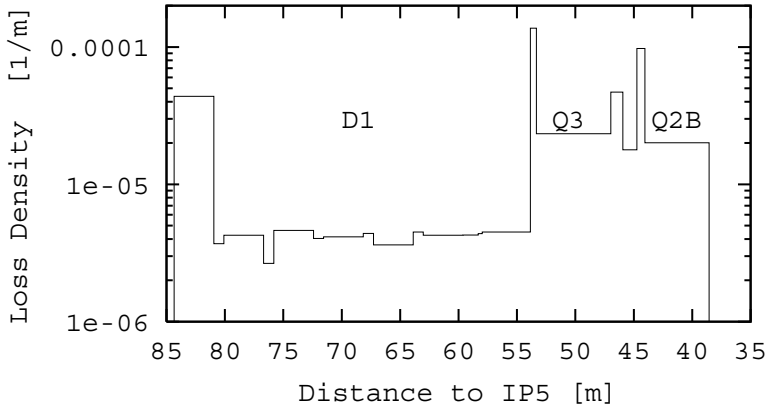

Figure 8 Loss densities upstream of IP5 along Beam1 for the nominal collision optics and fully open tertiary collimators. The corresponding integrated loss of $9.76 \cdot 10^{-4}$ can be compared with the loss of $2.44 \cdot 10^{-3}$ at the pair TCTH.4L5 and TCTV.4L5 when they are set to 8.3σ.

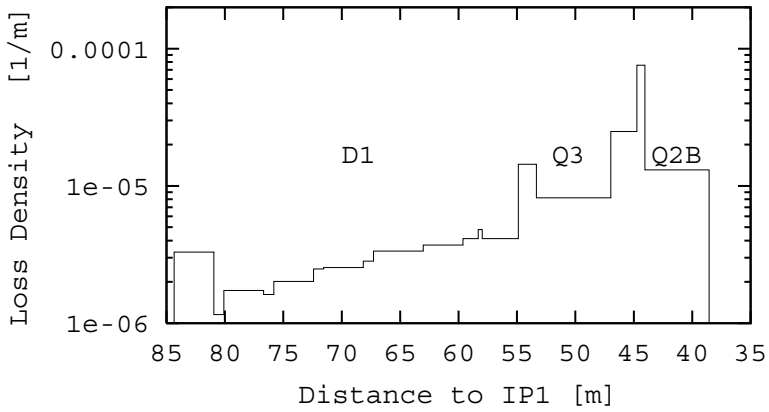

Figure 9 Loss densities upstream of IP1 along Beam 2 for the nominal collision optics and fully open tertiary collimators. The corresponding integrated loss of $3.83 \cdot 10^{-4}$ can be compared with the loss of $2.48 \cdot 10^{-3}$ at the pair TCTH.4R1 and TCTV.4R1 when they are set to 8.3σ.

The integrated losses upstream of the experiments are obviously lower than the losses at the corresponding tertiary collimators. This is the price paid for the triplets protection both upstream and downstream of the IP. The values of n_3 can be discussed of course in each individual case but all the loss sources including both cleanings and residual gas in the arcs must be taken into account.

5. Conclusion

Numerous results presented in this paper demonstrate the high efficiency of the baseline momentum collimation system at top energy. At the same time even the relatively small losses in the experimental insertions must be taken into account in the background studies along with the losses due to the betatron cleaning and beam-gas scattering.

Acknowledgements

The author would like to thank J.B. Jeanneret and T. Risselada for their continuous help and numerous discussions of the momentum cleaning and the features of the off-momentum optics.

References

[1] LHC Design Report – Volume 1: The LHC Main Ring, CERN Editorial Board, CERN-2004-003, 2004

[2] N. Catalan Lasheras, G. Ferioli, J.B. Jeanneret et al., Proton Collimation in TeV Colliders, LHC Project Report 156, 1997

[3] J.B. Jeanneret, Optics of a Two-Stage Collimation System, LHC Project Report 243, 1998

[4] D. Kaltchev, M. Craddock, R. Servranckx and T. Risselada, Momentum Cleaning in the CERN LHC, LHC Project Report 194, 1998

[5] J.B. Jeanneret, Specification for the Momentum Cleaning, LHC Project Note 115, 1997

[6] R. Assmann, D. Macina, K.M. Potter et al., Tertiary Halo and Tertiary Background in the Low Luminosity Experimental Insertion IR8 of the LHC, LHC Project Report 953, 2006

[7] I. Baishev, A. Barsukov and J.B. Jeanneret, Radiation Heating of Primary Collimators at Ramping, LHC Project Report 309, 1999

[8] I. Baishev, A. Drozhdin and N. Mokhov, STRUCT Code Reference Manual, SSCL-MAN-0034, 1994

[9] M. Lamont, Estimates of Annual Proton Doses in the LHC, LHC Project Note 375, 2005

Appendix

Losses at the machine elements in the Figures and in the Table below are given per one cleaning event so that the full loss per one beam is equal to 1.

a) nominal collision optics

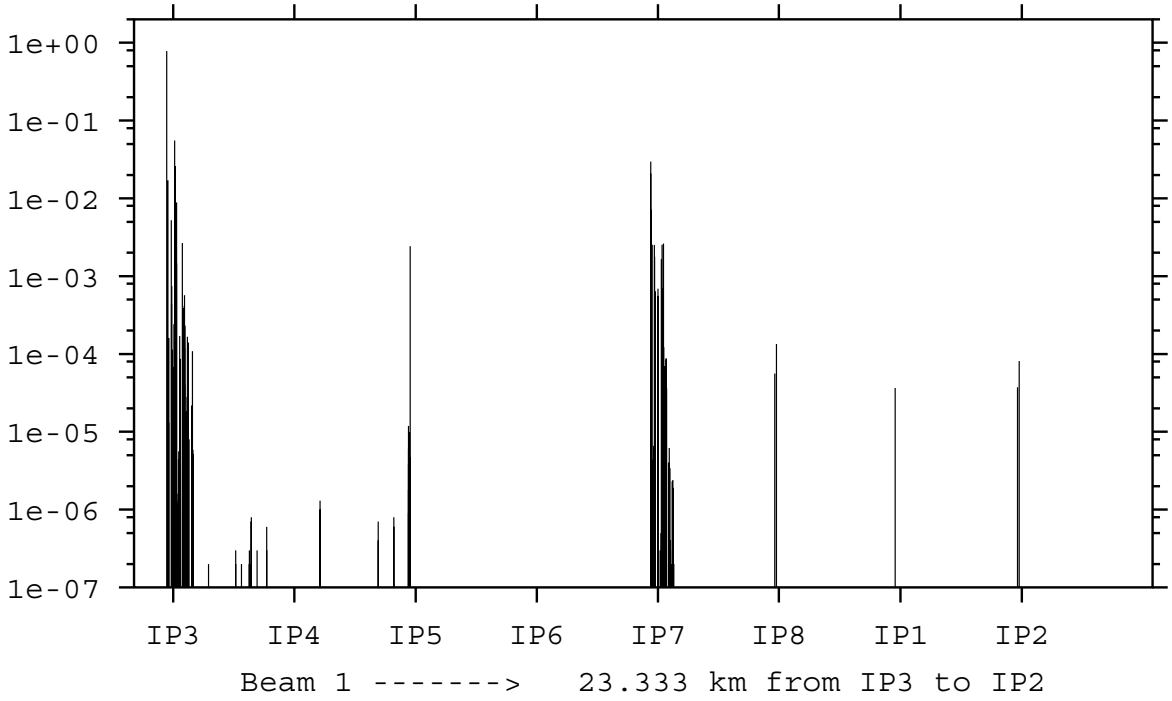

b) early collision optics

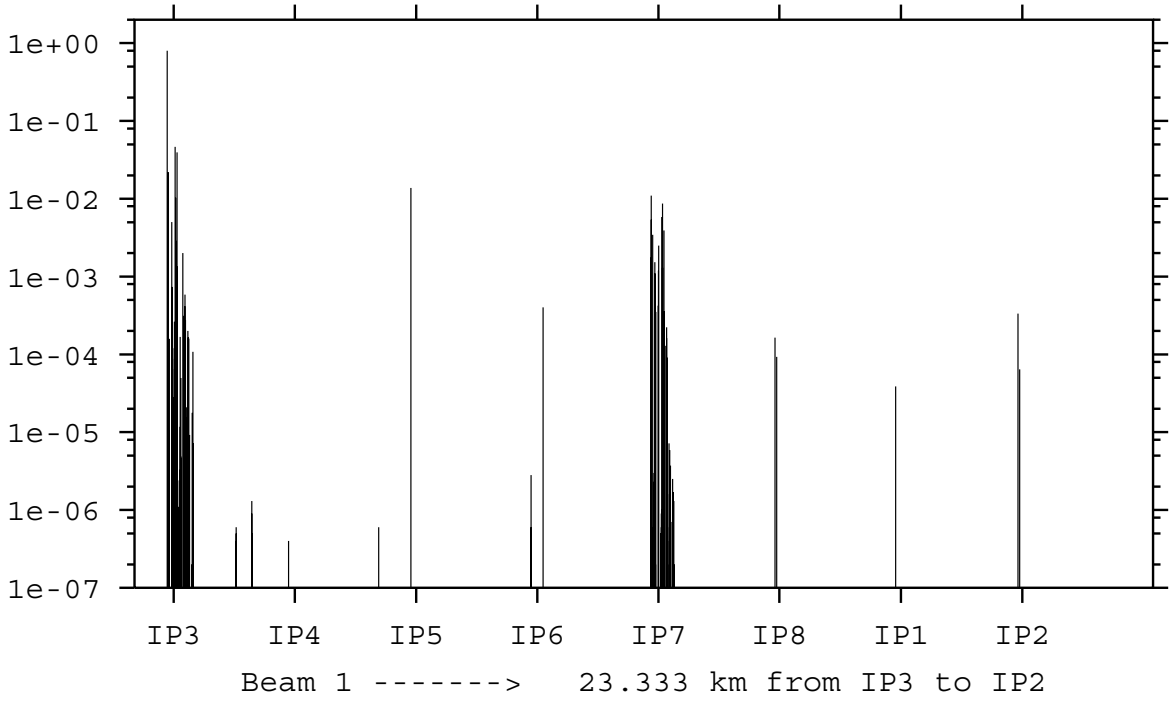

Figure A1 Losses along the Ring 1 of the LHC in the case of the tertiary collimators at 8.3σ: a) nominal collision optics, b) early collision optics.

a) nominal collision optics

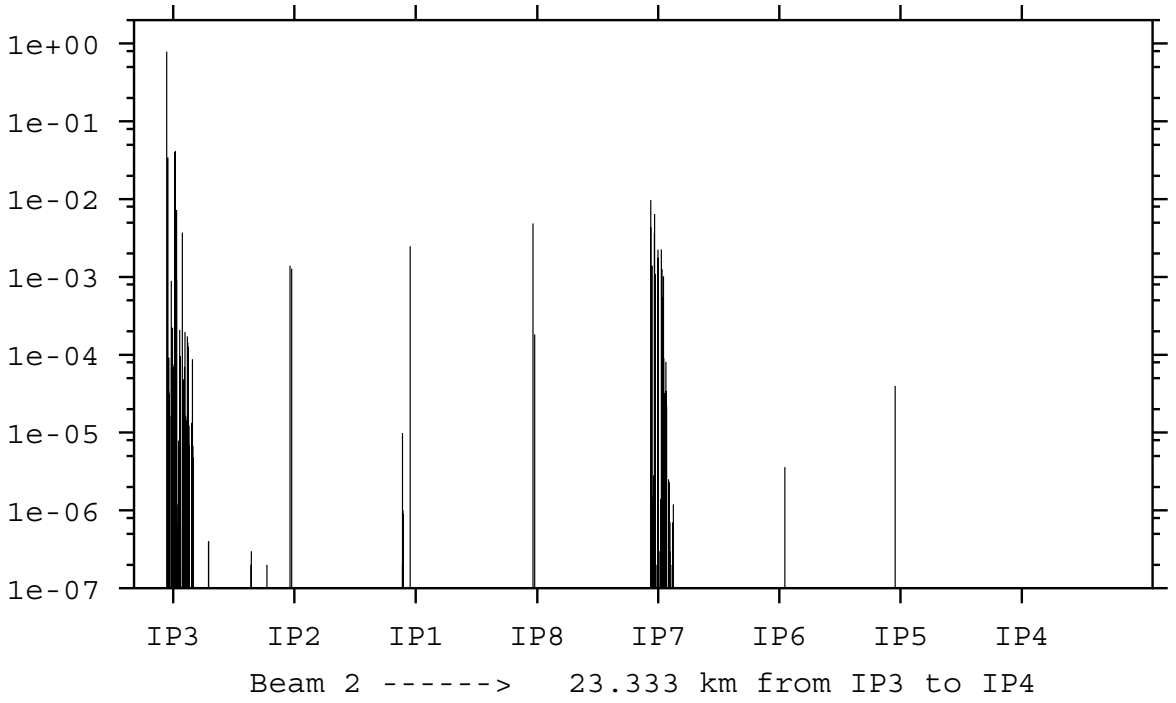

b) early collision optics

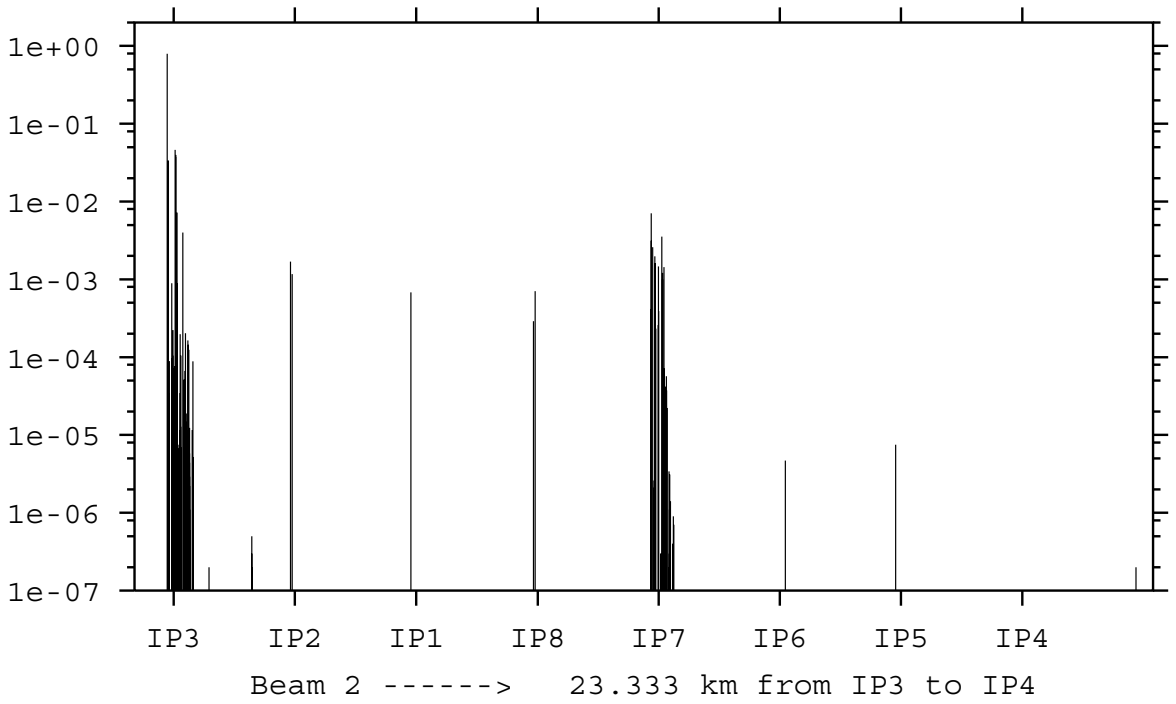

Figure A2 Losses along the Ring 2 of the LHC in the case of the tertiary collimators at 8.3σ: a) nominal collision optics, b) early collision optics.

a) nominal collision optics

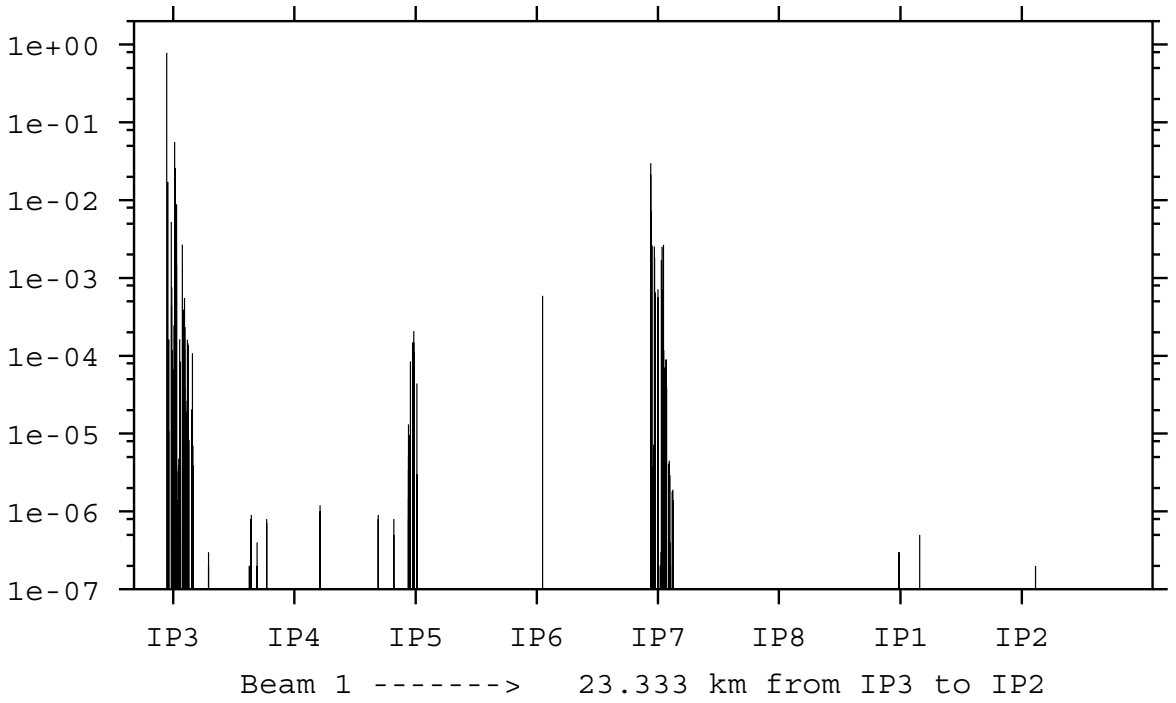

b) early collision optics

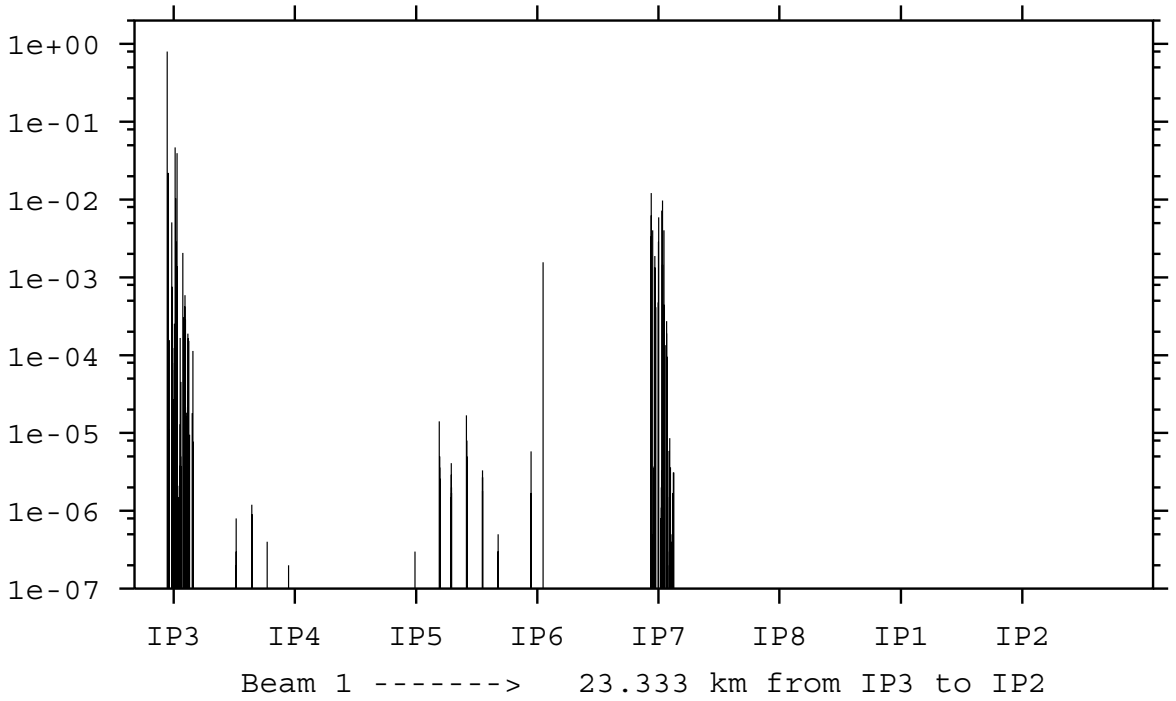

Figure A3 Losses along the Ring 1 of the LHC in the case of fully open tertiary collimators: a) nominal collision optics, b) early collision optics.

a) nominal collision optics

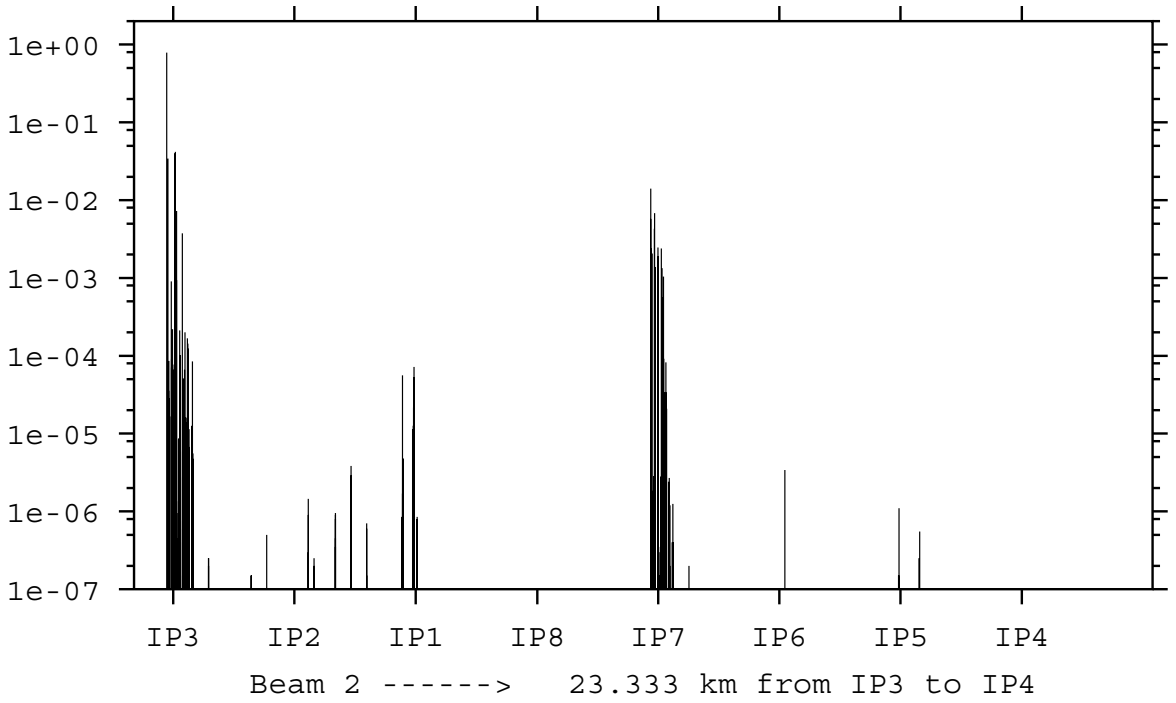

b) early collision optics

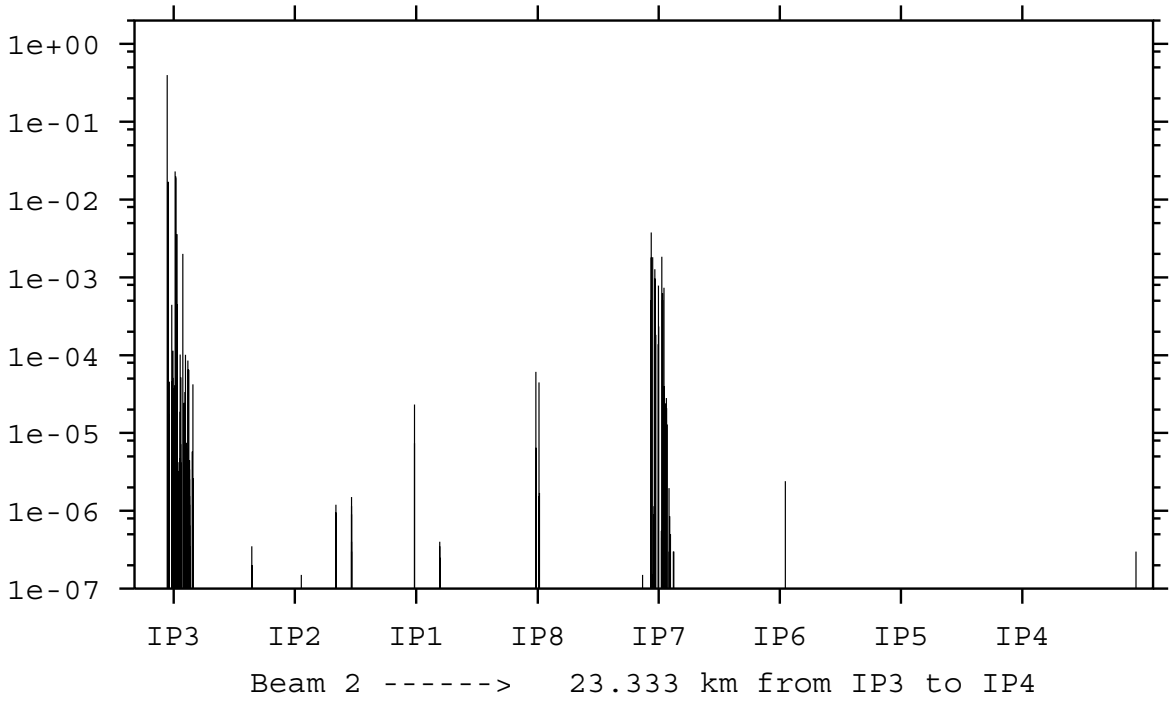

Figure A4 Losses along the Ring 2 of the LHC in the case of fully open tertiary collimators: a) nominal collision optics, b) early collision optics.

Table A1: Losses at the collimators in the two Rings for both the nominal and the early collision optics. The tertiary collimators (TCT) are at 8.3σ.

Ring 1	**optics**		**Ring 2**	**optics**	
	Nominal	**Early**		**Nominal**	**Early**
TCP.6L3	0.77997E+00	0.80028E+00	TCP.6R3	0.78532E+00	0.79586E+00
TCSG.5L3	0.17060E-01	0.22068E-01	TCSG.5R3	0.34247E-01	0.33840E-01
TCSG.4R3	0.55594E-01	0.46615E-01	TCSG.4L3	0.40178E-01	0.46014E-01
TCSG.A5R3	0.19957E-01	0.10298E-01	TCSG.A5L3	0.34785E-01	0.37622E-01
TCSG.B5R3	0.25963E-01	0.28717E-02	TCSG.B5L3	0.41695E-01	0.39611E-01
TCLA.A5R3	0.88774E-02	0.39506E-01	TCLA.A5L3	0.72502E-02	0.72142E-02
TCLA.B5R3	0.14535E-02	0.13445E-02	TCLA.B5L3	0.93290E-03	0.88940E-03
TCLA.6R3	0.17060E-03	0.16790E-03	TCLA.6L3	0.20830E-03	0.19750E-03
TCLA.7R3	0.26690E-02	0.20111E-02	TCLA.7L3	0.37298E-02	0.39971E-02
TCTH.4L5	0.13722E-02	0.12746E-02	TCTH.4R2	0.13961E-02	0.16961E-02
TCTV.4L5	0.10663E-02	0.12506E-01	TCTV.4R2	0.12791E-02	0.11661E-02
TCDQ.4R6	0.00000E+00	0.40210E-03	TCTH.4R1	0.10355E-02	0.55070E-03
TCP.D6L7	0.20749E-01	0.17658E-02	TCTV.4R1	0.14416E-02	0.12950E-03
TCP.C6L7	0.29708E-01	0.10972E-01	TCTH.4R8	0.48761E-02	0.29040E-03
TCP.B6L7	0.71443E-02	0.53730E-02	TCTV.4R8	0.18300E-03	0.70710E-03
TCSG.A6L7	0.25397E-02	0.34322E-02	TCP.D6R7	0.11894E-02	0.41750E-03
TCSG.B5L7	0.25157E-02	0.15307E-02	TCP.C6R7	0.97183E-02	0.70750E-02
TCSG.A5L7	0.17761E-02	0.10918E-02	TCP.B6R7	0.43634E-02	0.31445E-02
TCSG.D4L7	0.63720E-03	0.35060E-03	TCSG.A6R7	0.13918E-02	0.25946E-02
TCSG.B4L7	0.32850E-03	0.42280E-03	TCSG.B5R7	0.36680E-02	0.19809E-02
TCSG.A4L7	0.69040E-03	0.11970E-02	TCSG.A5R7	0.64578E-02	0.16206E-02
TCSG.A4R7	0.55840E-03	0.24998E-02	TCSG.D4R7	0.10971E-02	0.23270E-03
TCSG.B5R7	0.16412E-02	0.58091E-02	TCSG.B4R7	0.59760E-03	0.25870E-03
TCSG.D5R7	0.25345E-02	0.86643E-02	TCSG.A4R7	0.22520E-02	0.14647E-02
TCSG.E5R7	0.70610E-03	0.12958E-02	TCSG.A4L7	0.17585E-02	0.39040E-03
TCSG.6R7	0.26298E-02	0.39106E-02	TCSG.B5L7	0.22566E-02	0.35521E-02
TCLA.A6R7	0.12130E-03	0.35560E-03	TCSG.D5L7	0.12665E-02	0.12127E-02
TCLA.C6R7	0.70000E-04	0.12860E-03	TCSG.E5L7	0.54110E-03	0.99770E-03
TCLA.E6R7	0.85100E-04	0.22260E-03	TCSG.6L7	0.10205E-02	0.14347E-02
TCLA.F6R7	0.88600E-04	0.16220E-03	TCLA.A6L7	0.90200E-04	0.71300E-04
TCLA.A7R7	0.36000E-04	0.90800E-04	TCLA.C6L7	0.32200E-04	0.41900E-04
TCTH.4L8	0.56200E-04	0.16420E-03	TCLA.E6L7	0.81100E-04	0.56900E-04
TCTV.4L8	0.13460E-03	0.93200E-04	TCLA.F6L7	0.34400E-04	0.37300E-04
TCTH.4L1	0.25700E-04	0.81000E-05	TCLA.A7L7	0.21700E-04	0.22200E-04
TCTV.4L1	0.11000E-04	0.30500E-04	TCDQ.4L6	0.36000E-05	0.47000E-05
TCTH.4L2	0.37400E-04	0.33300E-03	TCTH.4R5	0.35600E-04	0.24000E-05
TCTV.4L2	0.80900E-04	0.64200E-04	TCTV.4R5	0.43000E-05	0.51000E-05
All@Beam1	0.98906E+00	0.98931E+00	All@Beam2	0.99644E+00	0.99640E+00